


## Article

# Biomass and Carbon Stock Quantification in Cork Oak Forest of Maamora Using a New Approach Based on the Combination of Aerial Laser Scanning Carried by Unmanned Aerial Vehicle and Terrestrial Laser Scanning Data

Fadil Sanaa <sup>1,2,\*</sup>, Sebari Imane <sup>1</sup> , Bouhaloua Mohamed <sup>3</sup>, Ait El kadi Kenza <sup>1</sup>, Kellouch Souhail <sup>4</sup>, Hamza Lfalah <sup>1</sup> and Meghraoui Khadija <sup>1</sup>

<sup>1</sup> Department of Cartography and Photogrammetry, School of Geomatics and Surveying Engineering, IAV Hassan II, Rabat 10000, Morocco; i.sebari@iav.ac.ma (S.I.); k.aitelkadi@iav.ac.ma (A.E.k.K.); hamza.falah2@gmail.com (H.L.); k.meghraoui@iav.ac.ma (M.K.)

<sup>2</sup> National Agency of Water and Forests, Rabat 10000, Morocco

<sup>3</sup> Department of Natural Resources and Environment, IAV Hassan II, Rabat 10000, Morocco; m.bouhaloua@iav.ac.ma.com

<sup>4</sup> AXIGEO Campanie, Marrakech 40000, Morocco; souhailkel@gmail.com

\* Correspondence: s.fadil@iav.ac.ma; Tel.: +21-2648-770-740

**Abstract:** The Mediterranean forests, particularly Cork oak (*Quercus suber* L., 1927), make a major contribution to the fight against climate change through Carbon sequestration. Hence, there is a great interest in the accurate quantification of biomass and carbon stock. In this context, this study aims at assessing the performance of a new approach, based on the combination of Unmanned aerial vehicle airborne Aerial laser scanning (ALS-UAV) and Terrestrial laser scanning (TLS) data, in the determination of dendrometric parameters (Circumference at 1.30 m and Tree Height), and consequently the estimation of biomass and carbon stock, considering field data as reference. This study takes the Maamora forest in Morocco as an example of a Mediterranean Cork oak forest. The methodology consists of collecting data at three levels: the entire area level for an ALS-UAV scan, the plot and tree levels for TLS surveys, as well as field data collection. Afterwards, dendrometric parameters (Circumference at 1.30 m and the Tree height) were estimated using individual tree segmentation and biomass; the carbon stock (aboveground, belowground, and total) was estimated using allometric equations. The comparison of the estimated dendrometric parameters with those measured in the field shows a strong relationship, with a Pearson coefficient of 0.86 and 0.83, a correlation coefficient ( $R^2$ ) of 0.81 and 0.71, and a Root mean square error (RMSE) of 1.84 cm and 0.47 m, respectively. Concerning the biomass and carbon stock estimation, the proposed approach gives a satisfactory accuracy, with a Pearson coefficient of 0.77, an  $R^2$  of 0.83, and an RMSE of 36.40 kg for biomass and 20.24 kg for carbon stock.

**Keywords:** biomass; carbon stock; combination of ALS-UAV and TLS data; segmentation tree; Mediterranean region; allometric equations; Cork oak forest



**Citation:** Sanaa, F.; Imane, S.; Mohamed, B.; Kenza, A.E.k.; Souhail, K.; Lfalah, H.; Khadija, M. Biomass and Carbon Stock Quantification in Cork Oak Forest of Maamora Using a New Approach Based on the Combination of Aerial Laser Scanning Carried by Unmanned Aerial Vehicle and Terrestrial Laser Scanning Data. *Forests* **2022**, *13*, 1211. <https://doi.org/10.3390/f13081211>

Academic Editor: Jan Bocianowski

Received: 5 June 2022

Accepted: 25 July 2022

Published: 1 August 2022

**Publisher's Note:** MDPI stays neutral with regard to jurisdictional claims in published maps and institutional affiliations.



**Copyright:** © 2022 by the authors. Licensee MDPI, Basel, Switzerland. This article is an open access article distributed under the terms and conditions of the Creative Commons Attribution (CC BY) license (<https://creativecommons.org/licenses/by/4.0/>).

## 1. Introduction

Terrestrial ecosystems, such as forests and soils, sequester and store globally critical stocks of carbon, but they are threatened by deforestation and Climate change [1]. In fact, the CO<sub>2</sub> sink in these ecosystems increased from  $1.3 \pm 0.4 \text{ GtC yr}^{-1}$  in the 1960s to  $3.4 \pm 0.9 \text{ GtC yr}^{-1}$  from 2010–2019, with important inter-annual variations of up to  $2 \text{ GtC yr}^{-1}$  [2]. Forest ecosystems are the largest part of terrestrial ecosystems [3,4], containing about 80% of aboveground carbon and 40% of belowground terrestrial carbon [5]. On the one hand, terrestrial ecosystems contribute to the mitigation of ~31% of global emissions from land use change and fossil-fuel burning [2]. On the other hand, forest degradation

and deforestation are leading to carbon dioxide (CO<sub>2</sub>) emissions and the worsening of global Climate change [6]. In fact, degraded forests contained 45.1% of the carbon stocks in intact forests, and these differences persisted even after 15 years of regrowth [7]. Thus, the tree biomass and the rate of carbon sequestration decreased from undisturbed to degraded forests by 62% and 73%, respectively [8].

In the Mediterranean region, carbon sequestration by forests ranges between 0.01 and 1.08 t C /hectare annually [9]. *Quercus suber* L., 1927 or Cork Oak forests are among the most important Mediterranean forest stands. They provide several environmental, economic, and social functions and they widely contribute to the fight against climate change.

Aboveground biomass (AGB) is a major component of the terrestrial carbon cycle, and its accurate estimation is critical for supporting policies of ecosystem conservation and Climate change mitigation [10]. It is a sensitive indicator of environmental change and ecological functions [11]. The carbon captured (or stored) by a tree is the amount of carbon accumulated in its biomass. It is expressed in kg/tree and by geographical area (ton/hectare and ton/hectare/tree).

Carbon stock and biomass quantification are crucial in environmental fields, but they are also constraining at the same time, especially in large areas. In fact, biomass estimation is especially important for arid and semiarid regions, which are particularly susceptible to environmental degradation and desertification [12]. Forest biomass can be estimated through field measurements. Two methods are available: a destructive one, also known as the harvest method, and a non-destructive method using allometric equations [13].

Although the field measurements provide a more accurate estimation of forest biomass, they are labor intensive as well as time-consuming and rather expensive. In addition, the manual collection of the biometrical data of Cork oak trees is difficult due to their varied architecture. However, the estimation of their aboveground biomass and carbon stock with remote sensing provides a reasonable alternative, saving time and effort.

Remote sensing is recognized as an effective tool for quantifying carbon stocks over large areas, enabling accurate monitoring at the landscape scale [13,14]. Several researchers have studied the use of remote sensing tools in this field, such as aerial photos [15], Landsat image data [16,17], imaging spectrometry [18], hyperspectral imaging (HSI), and very high-resolution data [19,20]. However, the use of satellite imagery in AGB and carbon stock estimation is limited because it cannot capture the sub-canopy properties of vegetation.

Hence the interest of using Aerial Laser Scanning (ALS), which characterizes complex forest structures due to its ability to capture three-dimensional information of the land surface [21] and reduce the cost of obtaining AGB and carbon stock estimation to a specific level [22]. Many researchers have used ALS alone [23] or combined with other remote sensing tools to estimate the aboveground biomass and the carbon stock in many forests all around the world. ALS has been used with Landsat 8 OLI (Operational Land Imager) data and allometric equations to derive mangroves' height, biomass, and carbon stock in north-western Australia [24], and with Sentinel-2 imagery, using a new upscaling method to estimate the AGB in a Mangrove Forest [25]. ALS and hyperspectral data used separately yield good results and their combination provides more accurate AGB estimations [26].

In addition to the estimation of biomass and carbon stock at a given time, some studies have focused on the use of ALS in combination with ancillary remote sensing tools to explore temporal changes in forest cover and degradation aspects. In fact, ALS data were used with forest inventory data to quantify the aboveground carbon density (ACD) in intact and degraded forests [27]. High density ALS data and Landsat imagery time series were used to investigate the forest degradation caused by logging and fire [7]. Landsat-derived tree canopy cover, height, intactness, and forest cover loss and The Geoscience Laser Altimeter System (GLAS) Lidar-derived forest biomass were used to estimate the tropical forest aboveground carbon (AGC) loss from 2000 to 2012 [28]. In addition, ALS and Landsat Imagery Data were used to study the changes in vegetation cover and to quantify its impact on aboveground carbon (AGC) stocks in Auckland, New Zealand, between 1989 and 2014 [29].

ALS can be carried by different platforms; in particular, Unmanned Aerial Vehicles (UAVs), which have recently proven their efficiency in forest resource investigation and data acquisition, possess much higher spatial and temporal resolutions than other remote sensing tools [30]. In addition to UAV-based Lidar (ALS-UAV), many researchers have experimented the use of UAV imagery for aboveground biomass and carbon stock estimation. For this purpose, a cost-effective method integrating UAV-imagery and Terrestrial Laser Scanning (TLS) data was deployed in a tropical rainforest in Malaysia [31]; a combined field and object-based image analysis (OBIA) approach, based on UAV multispectral imagery, was used in a Mediterranean Riparian Forest [32]; and aerial photos from a UAV were used to estimate the aboveground biomass and carbon Stock in the Karimunjawa-Kemujan Islands [33].

In addition to Aerial Laser Scanning (ALS), Terrestrial Laser Scanning (TLS) has been used in several forestry studies, notably in the estimation of the dendrometric parameters of trees and their aboveground biomass and carbon stock [32].

New technologies have been widely tested in several forests throughout the world; however, few studies have concerned Mediterranean forests and in particular Cork oak forests. Indeed, these forests present an exceptional natural setting and greatly contribute to the sustainable development of the area. Hence the importance of appropriate and simplified management, involving innovative technologies such as UAV, ALS, and TLS.

This study assesses the performance of using a new approach, based on the combination of Unmanned Aerial Vehicle airborne Aerial Laser Scanning (ALS-UAV) and Terrestrial Laser Scanning (TLS) data, towards the determination of dendrometric parameters (C1.30m and Tree Height) and consequently the estimation of biomass and carbon stock, considering field data as reference.

The specific objectives are:

- To assess the potential of estimating trees' attributes (C1.30m and Tree Height) based on the combination of ALS-UAV and TLS data, and to compare it with the dendrometric parameters measured in the field.
- To estimate tree biomass and biomass at the plot level; then, to assess their accuracies by comparing them with the biomass estimated based on the dendrometric parameters measured in the field.
- To calculate the carbon stock at the tree and plot levels with ALS-UAV-TLS data and to study their precision in comparison to the field data.

This paper is organized as follows: In Section 2, we describe the methodological approach, starting with describing the study area, detailing the data acquisition, preprocessing, processing, biomass, and carbon stock estimations, followed by a statistical analysis. The results are then presented in Section 3 and discussed in Section 4.

## 2. Materials and Methods

The methodology of this research work is organized in three stages: firstly, the data acquisition, which was carried out at three levels (ALS-UAV acquisition, TLS acquisition, and field data acquisition); secondly, preprocessing, processing, biomass, carbon stock estimation; and thirdly, a statistical analysis, which assessed the relationship between field-measured variables and those extracted from ALS-UAV-TLS data (Figure 1).

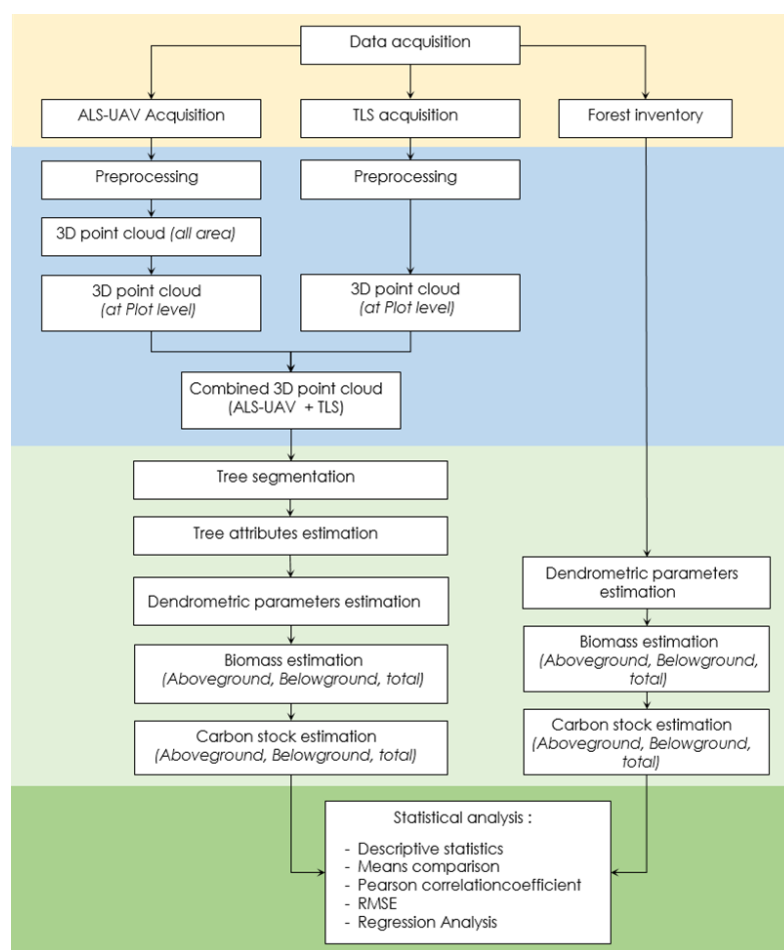


**Figure 1.** Flowchart of the research method.

### 2.1. Study Area

This study is conducted in a Mediterranean Cork oak forest, located in Maamora forest in Morocco (Figure 2). This forest is considered the largest Cork oak forest in the world [34]. It is spread over 131,921 ha [35], of which 60,000 ha consists of pure Cork oak stand, and it is sectioned from west to east in five cantons: A, B, C, and D. This area is characterized by a sub-humid bioclimate in its western part and is semi-arid in its central and eastern parts. The tree layer vegetation is marked by almost pure Cork oak (*Quercus suber*) [36].

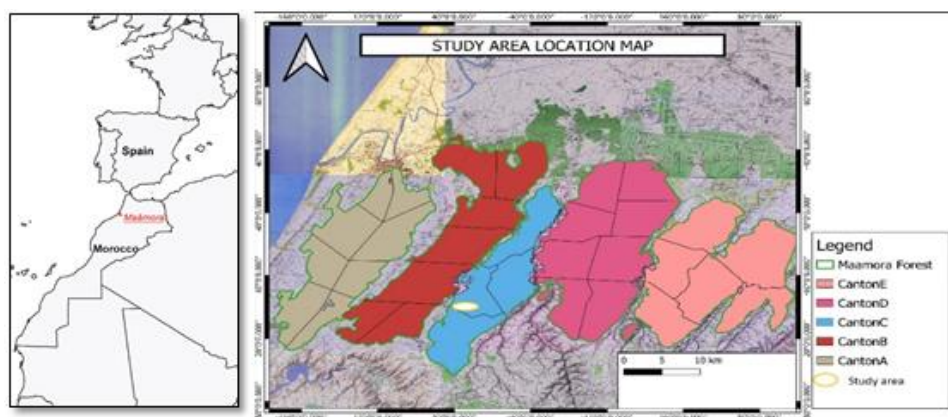


**Figure 2.** Location of Maamora forest.



The Maamora forest greatly contributes to local and regional development. Its socioeconomic and environmental roles are of great importance. Nevertheless, she is under very strong anthropogenic pressure due to the appropriation of timber for various uses, overgrazing, and the systematic collection of sweet acorns for local consumption and marketing. These destructive practices, which exacerbate the weaknesses caused by the forests senescence, render it very vulnerable [37]. The present study was conducted in the central canton C, group III, parcel 10, inside a pure adult Cork oak stand with a density less than 100 stem/ha.

## 2.2. Data Acquisition

### 2.2.1. ALS-UAV Data Acquisition

Before The ALS-UAV mission, we explored the study area, looking for reference points and preparing the equipment. The choice of the reference points found in planimetry (ITRF and Merchich) and altimetry (NGM) was made after performing homogeneity tests. After that, the mission planning was carried out to set flight parameters. Then, the ALS-UAV data were collected on 17 July 2020, with Velodyne VLP-16 Lidar sensor mounted on an Unmanned Aerial Vehicle DJI Matrice 600 pro (Figure 3). This sensor has an effective range of 75 m, a point accuracy up to 3 cm, and a data rate of 300,000 points per second. The height of flight was 40 m with a speed of 3 m/s and a side overlap of 30%. The area covered by the mission is about 10 ha.

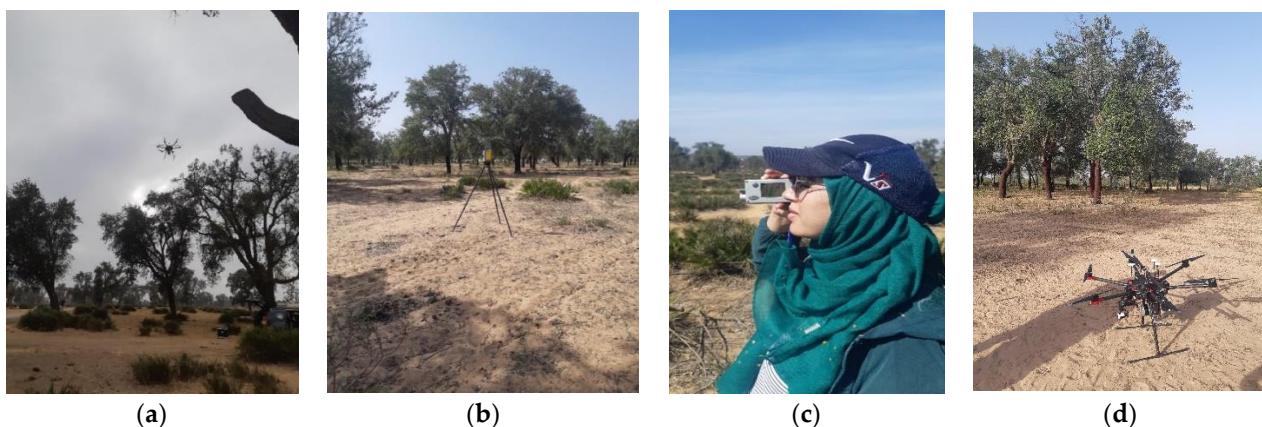


**Figure 3.** (a) ALS-UAV Data Acquisition; (b) Data acquisition with Trimble X7 scanner; (c) Tree height acquisition with Vertex Hypsometer (d) Velodyne VLP-16 Lidar sensor on Matrice 600 pro UAV.

### 2.2.2. TLS Data Acquisition

The data survey with TLS was performed using a multiscan configuration with four scan stations (Figure 4). The first scan position was at the center of the plot and the other three scans were conducted on the border separated by an angle of 120 degrees. In the field, these scans were operated one after another. The multiple scan approach can reduce the problem of occlusion, which is caused by tree stems, branches, or other forms of understory vegetation near the scanner's location [38]. The acquisition of the TLS data was performed by a Trimble X7 scanner (Figure 3). Before carrying out the scans, the target points (reference retro-reflectors) were installed on the ground and their positions were collected by the Comnav T300 GNSS receiver. These points are important for accurately co-registering and geo-referencing the four separate scans of the plot.

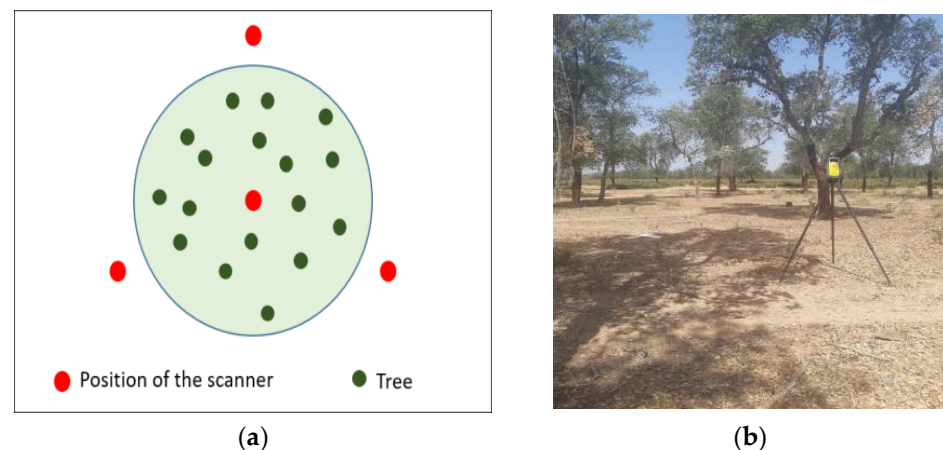


**Figure 4.** (a) Configuration of the Terrestrial laser scanner (TLS) multiscan; (b) Terrestrial laser scanner (TLS) operating a scan on the border of the plot.

### 2.2.3. Field Data Collection

Field measurements were taken to provide a basis for comparing the ALS-UAV-TLS data. In effect, we used a sampling plan of data acquisition on six randomly distributed plots. The latter plots were circular with a radius of 20 m and each one covering 1256 m<sup>2</sup>.

For every plot, we measured the circumference at 1.30 m aboveground for all existing trees (67 trees) using measuring tape. Then, we randomly selected sample trees (38 trees), for which we measured the total height using a Vertex Hypsometer (Figure 3) and the circumference at 1.30 m from the ground using circumference tape.

## 2.3. Data Processing

### 2.3.1. ALS-UAV-TLS Data Pre-Processing and Processing

Before using the point cloud, a pre-processing step is necessary. It consists of three main steps, automatic consolidation to group all the clouds from the different stations together, geo-referencing to position the spatial entities in a specific coordinate system, and noise cleaning to eliminate points. Once the TLS and ALS point clouds are pre-processed, the resulting files are combined. The combined file follows a workflow pattern to extract tree attributes or dendrometric parameters (Figure 5).

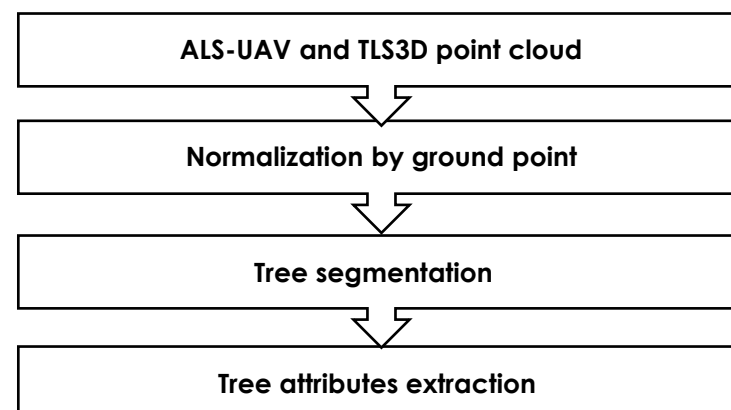


**Figure 5.** Processing steps of ALS-UAV and TLS 3D point cloud.

- Normalization by ground point

Normalization of the point cloud (Figure 6) removes the effects of topographic relief on the elevation values of the point cloud data. This operation requires the input data to have already been classified into ground points and non-ground points. The normalization

process is performed by subtracting the elevation of the terrain (represented by the elevation of the ground points) of the Z value of each point.

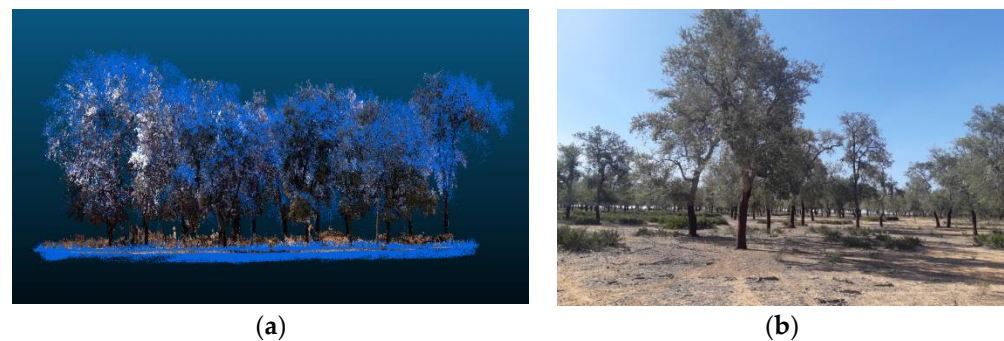


**Figure 6.** (a) 3D plot point cloud ALS-UAV-TLS in Maamora forest; (b) Cork oak stand in Maamora.

- Tree segmentation

The point cloud segmentation method uses shortest-path algorithm (CSP), which can segment both broadleaved and coniferous forests scanned using T-Lidar and trees scanned using mobile Lidar [39]. This algorithm functions via two steps: firstly, the trunk detection, and secondly, the subsequent crown segmentation, and it presents a high accuracy in terms of the number of detected trees and crown segmentation. Individual Tree attributes, including Tree height and Diameter at Breast Height (DBH), can be then determined for each Tree segmented out of the inputs' TLS dataset.

- Tree attributes extraction

Point cloud segmentation tool generates a file containing tree attributes for all trees' ID records including: location (x,y), tree height, crown diameter, crown area, crown volume, and DBH, which is closely related to circumference at 1.30 m (C1.30m). The latter is calculated by multiplying the DBH by  $\pi$  (3.14).

### 2.3.2. Field Data Processing

The processing of field data concerns the study of the relationship between the circumference at 1.30 m and the heights of trees. This relationship is studied by simple modeling using R software. The resulting model allowed us to calculate the total height of all trees in the study area.

- Model Specifications:

To study the relationship between the tree height and the circumference at 1.30 m from the ground, we tested the six following mathematical models from observations collected in the field (Table 1):

**Table 1.** Models used to characterize relationship between tree height and circumference at 1.30 m. Where H is the tree height and C1.30 m is the circumference of tree at 1.30 m from the ground.

Models	Models' Equations
Model 1	Linear simple model: $H = b_0 + b_1 C_{1.30m}$
Model 2	Allometric model (2nd degree): $H = b_0 + b_1 C_{1.30m} + b_2 C_{1.30m}^2$
Model 3	Allometric model (3rd degree): $H = b_0 + b_1 C_{1.30m} + b_2 C_{1.30m}^2 + b_3 C_{1.30m}^3$
Model 4	Allometric model (4th degree): $H = b_0 + b_1 C_{1.30m} + b_2 C_{1.30m}^2 + b_3 C_{1.30m}^3 + b_4 C_{1.30m}^4$
Model 5	Allometric model (5th degree): $H = b_0 + b_1 C_{1.30m} + b_2 C_{1.30m}^2 + b_3 C_{1.30m}^3 + b_4 C_{1.30m}^4 + b_5 C_{1.30m}^5$
Model 6	Logarithmic model: $\ln H = a_0 + a_1 \ln C_{1.30m}$

- Criteria for choosing models

The best model is the one that satisfies the following conditions:

1. Multiple and adjusted  $R^2$ —Coefficient of determination is the proportion of the variation in the dependent variable that is predictable from the independent variable(s).
2. Residual standard error—The mean square error is the mean of the sum of squared residuals; it measures the average of the squares of the errors. Lower values (closer to zero) indicate better fit.
3. AIC—The Akaike information criterion is an estimator of prediction error and thereby relative quality of statistical models for a given set of data.
4. BIC—Bayesian information criterion (BIC) is a criterion for model selection among a finite set of models; models with lower BIC are generally preferred.

#### 2.4. Biomass and Carbon Stock Estimation

To estimate biomass and carbon stock, we have used two methods: the first method is based on data from the field survey inputs and the second one is based on ALS-UAV-TLS data inputs. Then, the allometric equations explained in the following sections were used.

##### 2.4.1. Biomass Estimation

- Biomass estimation of Stem, Coarse branches, and Cork

To calculate the biomass of the stem, coarse branches, and the cork of the trees studied and in the absence of direct equations, we used volume equations established in the same forest on the basis of 34 trees representative of all stands in Maamora. As Moroccan law does not allow trees to be sampled destructively in the protected cork oak stands, an indirect method of geometrical cubing was used [40].

We first calculate the volume of the tree (Equation (A1)) and then the volume of the cork and the stem with coarse branches (Equations (A2) and (A3)) based on equations established from nearby Cork oak forests [41]. Then, the biomass is obtained by multiplying the volume of each component by the specific tissue density (Equations (A4) and (A5)) (Table A1).

- Biomass estimation of medium and small branches and foliage

Concerning medium and small branches and foliage, we directly calculated the biomass based on Equations (1) and (2) from a comparable ecosystem in Spain [42].

$$B_{\text{medium-branch}} = 0,127 \times D_{130} \times H \quad (1)$$

$$B_{\text{small-branch-foliage}} = 0,0463 \times D_{130} \times H \quad (2)$$

where  $D_{130}$  is the diameter at breast height (in cm),  $H$  is the tree height (in m),  $B_{\text{medium-branch}}$  is the biomass of medium branches (diameter 2–10 cm) in kg, and  $B_{\text{small-branch-foliage}}$  is the biomass of small branches (<2 cm diameter) and foliage (kg).

- Aboveground, belowground, and total biomass estimation

The estimation of Belowground biomass of each tree was determined based on Equation (A6) [42]. Then, the aboveground and total biomasses were calculated (Equations (3) and (4)).

$$B_{\text{tree-AGB}} = B_{\text{stem-bigB}} + B_{\text{cork}} + B_{\text{medium-branch}} + B_{\text{small-branch-foliage}} \quad (3)$$

$$B_{\text{tree-Total}} = B_{\text{tree-BLG}} + B_{\text{tree-AGB}} \quad (4)$$

where  $B_{\text{tree-AGB}}$  is the tree's aboveground biomass (in kg) and  $B_{\text{tree-Total}}$  is the total biomass of an individual tree in kg,  $B_{\text{tree-BLG}}$  is the belowground biomass of an individual tree in kg,  $B_{\text{cork}}$  is the biomass of cork (kg), and  $B_{\text{stem-bigB}}$  is the biomass of the stem and coarse branches without bark (kg).



The field plot biomass in (kg/ha) is obtained by first summing the biomass of all trees and then dividing the total by the area of the field plot; then, we convert it into Mg/ha (Equation (5)).

$$B_{\text{plot}} = \sum B_{\text{tree-Total}} / \text{Area}_{\text{plot}} \quad (5)$$

where  $B_{\text{plot}}$  is the biomass at the plot level in kg/ha,  $B_{\text{tree-Total}}$  is the total biomass of an individual tree in kg, and  $\text{Area}_{\text{plot}}$  is the area of the sample plot in ha.

#### 2.4.2. Carbon Stock Estimation

To calculate the carbon stock contained in each part (aboveground and belowground) of the cork oak tree, we multiply the correspondent biomass by the mean carbon concentration and by a conversion factor (Equation (6)), and then the total carbon stock corresponds to the sum of the aboveground and belowground carbon stock (Equation (7)).

$$C_{\text{st-part}} = \sum 10^{-3} (B_{\text{tree-part}} \times C_{\text{conc-part}}) \quad (6)$$

where  $C_{\text{st-part}}$  is the aboveground or belowground carbon stock (in kg) for  $n$  individual trees,  $10^{-3}$  is a conversion factor,  $B_{\text{tree-part}}$  is the aboveground or belowground biomass (in kg), and  $C_{\text{conc-part}}$  is the mean carbon concentration of the respective aboveground or belowground tissues (in  $\text{g kg}^{-1}$ —values from Table A1).

$$C_{\text{st-total}} = \sum (C_{\text{st-AGB}} + C_{\text{st-BLG}}) \quad (7)$$

where  $C_{\text{st-total}}$  is the total carbon stock content in the Cork oak tree (in kg),  $C_{\text{st-AGB}}$  is the aboveground carbon stock (in kg), and  $C_{\text{st-BLG}}$  is the Belowground carbon stock (in kg).

The field plot carbon stock in (kg/ha) is obtained by first summing the carbon stock of all trees and then dividing the total by the area of the field plot; then, we convert it into Mg/ha (Equation (8)).

$$C_{\text{plot}} = \sum C_{\text{st-total}} / \text{Area}_{\text{Plot}} \quad (8)$$

where  $C_{\text{plot}}$  is the carbon stock at the plot level in kg/ha,  $C_{\text{tree-Total}}$  is the total carbon stock of an individual tree in kg, and  $\text{Area}_{\text{plot}}$  is the area of the sample plot in ha.

#### 2.5. Statistical Analysis

In this study, we used descriptive statistics to describe variables of ALS-UAV-TLS data and field data. Then, to compare the means of variables with the two methods (field survey and ALS-UAV-TLS data), we have firstly examined the normality of data with Shapiro–Wilk test, and secondly applied the Wilcoxon test to compare means. Then, to understand the relationship between Field and ALS-UAV-TLS variables, we used Pearson Coefficient of Correlation, which measures the statistical relationship, or association, between two continuous variables, and Coefficient of Determination ( $R^2$ ), which shows the percentage of variation in one variable associated to other variables and can be explained by the given regression. In addition, the Root Mean Error Square (RMSE) (Equation (9)), is used to represent the performance of the model to explain the deviation between the measured variables (field data) and those estimated (ALS-UAV-TLS data). Then, to assess the relationship between field-measured variables and those extracted from ALS-UAV-TLS data, we used linear regression with a logarithmic transformation.

$$\text{RMSE} = \sqrt{\frac{1}{n} \sum_{i=1}^n (\hat{y}_i - y_i)^2} \quad (9)$$

where  $n$  is the number of measurements,  $y_i$  is the value of the  $i$ th observation in the validation dataset, and  $\hat{y}_i$  is the predicted value for the  $i$ th observation

### 3. Results

#### 3.1. Relationship between Tree Height and Circumference at 1.30 m

To characterize the relationship between the tree height and circumference at 1.30 m aboveground, three types of models (six equations) were used: a simple linear model, an allometric model (1st, 2nd, 3rd, 4th, and 5th degrees), and a linear model with a logarithmic transformation.

The criteria for choosing the right model linking the dependent variable “Tree height” to the explanatory variable “Circumference at 1.30 m” used in this study are: the  $R^2$ , Residual standard error, AIC, and BIC. The table below (Table 2) show models N° 1, 2, 3, 4, 5, and 6, along with their evaluation criteria.

**Table 2.** Models N° 1, 2, 3, 4, 5, and 6, with their evaluation criteria.

Models	Multiple $R^2$	Adjusted $R^2$	Residual Standard Error	AIC	BIC
Model 1—Linear simple model	0.66	0.65	1.198	130.40	125.48
Model 2—Allometric model (2nd degree)	0.67	0.65	1.194	126.20	132.75
Model 3—Allometric model (3rd degree)	0.71	0.68	1.147	124.04	132.23
Model 4—Allometric model (4th degree)	0.73	0.69	1.124	123.38	133.21
Model 5—Allometric model (5th degree)	0.75	0.71	1.087	121.63	133.09
Model 6—Logarithmic model	0.66	0.65	0.098	−64.47	−59.55

Based on the evaluation criteria, the best model is N° 6, which is the model with a logarithmic transformation, because it represents the lower Residual standard error, AIC, and BIC. The tree height of all trees in the study area was then calculated with the logarithmic model (Model 6):

$$\text{Log } H = 2.01285 + 0.63842 \text{ Log } C_{1.30\text{m}} \text{ (Model 6)}$$

#### 3.2. Statistical Analysis, Relationship, and Regression of Tree Dendrometric Parameters, Biomass, and Carbon Stock

In this section, we compare the dendrometric parameters, biomass, and carbon stock measured and calculated from the field measurements and those estimated from the ALS-UAV-TLS data at tree level. In the first level, we present the descriptive statistics. In the second one, we compare the means by studying the data distribution and performing the Wilcoxon–test. In the third level, we analyze the relationship between the data of the two methods by the Pearson correlation coefficient, RMSE, and the Regression analysis.

##### 3.2.1. Statistical Analysis and Comparison of Means

- Dendrometric parameters ( $C_{1.30\text{m}}$  and Tree Height)

The results of the descriptive statistics show that the averages of the dendrometric parameters are generally close. In fact, the average circumference at 1.30 m obtained from the field data collection was 94.16 cm and that obtained by the ALS-UAV-TLS data was 92.32 cm (Table 3). In addition, for the heights of the trees, the values 10.55 m and 10.08 m (Table 3) were recorded for the field and the ALS-UAV-TLS data, respectively. The other descriptive statistics concerning the height and circumference at 1.30 m of the trees obtained by the two methods are shown in Table 3 and illustrate in Figure 7.

To compare the means, we first study the distribution of data and then compare the means with the appropriate test. The representation by histograms, show that distributions of tree height and circumference at 1.30 m measured by field data collection and the circumference at 1.30 m extracted from UAV-ALS-TLS data, do not seem to follow a normal distribution, except tree height extracted from UAV-ALS-TLS data (Figure 8).

**Table 3.** Descriptive statistics of dendrometric parameters ( $H$ ,  $C_{1.30m}$ ), biomass, and carbon stock (aboveground, belowground, and total) measured and estimated with field data collection and from UAV-ALS-TLS data. Where,  $B_{tree-AGB}$  is the tree aboveground biomass (in kg),  $B_{tree-BLG}$  is the belowground biomass of an individual tree in kg,  $B_{tree-Total}$  is the total biomass of an individual tree in kg,  $C_{st-AGB}$  is the aboveground carbon stock (in kg),  $C_{st-BLG}$  is the carbon stock in the belowground tissues, and  $C_{st-total}$  is the total carbon stock content of an individual tree in kg.

		Min	1st Qu	Median	Mean	3rd Qu	Max
C 1.30m (cm)	Field measurements	50.00	74.75	90.00	94.16	108.50	202.00
	ALS-UAV-TLS	41.76	71.46	90.12	92.32	106.05	195.94
Height field (m)	Field measurements	8.10	9.45	10.69	10.55	11.77	14.36
	ALS-UAV-TLS	5.07	8.89	10.30	10.08	11.17	14.73
$B_{tree-AGB}$ field (kg)	Field measurements	145.5	336.1	506.9	619.9	759.8	2826.9
	ALS-UAV-TLS	87.81	306.20	474.54	586.80	729.20	2609.16
$B_{tree-BLG}$ field (kg)	Field measurements	21.02	46.98	68.11	81.75	98.98	343.08
	ALS-UAV-TLS	14.66	42.94	68.28	78.46	94.56	322.79
$B_{tree-total}$ field (kg)	Field measurements	166.5	383.1	575.0	701.7	858.8	3169.9
	ALS-UAV-TLS	102.5	348.7	542.8	665.3	825.1	2932.0
$C_{st-AGB}$ field (kg)	Field measurements	80.96	187.34	282.68	345.86	423.89	1579.41
	ALS-UAV-TLS	48.89	170.62	264.74	327.39	406.82	1457.79
$C_{st-BLG}$ field (kg)	Field measurements	11.35	25.37	36.78	44.14	53.45	185.26
	ALS-UAV-TLS	7.91	23.18	36.87	42.36	51.06	174.30
$C_{tree-total}$ field (kg)	Field measurements	92.31	212.71	319.46	390.00	477.34	1764.68
	ALS-UAV-TLS	56.81	193.59	301.61	369.75	458.60	1632.10

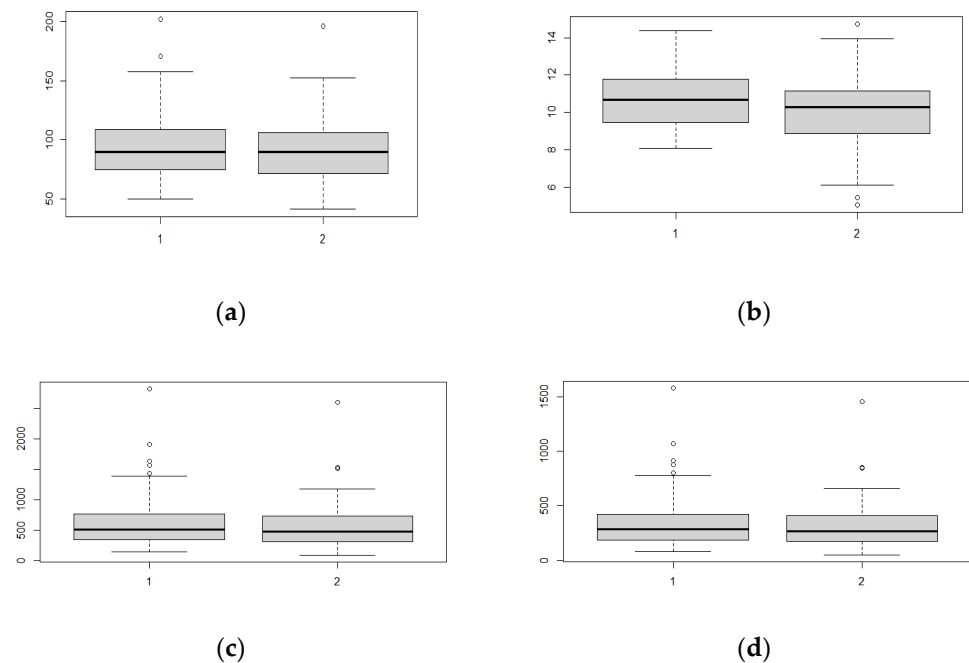


**Figure 7.** Cont.

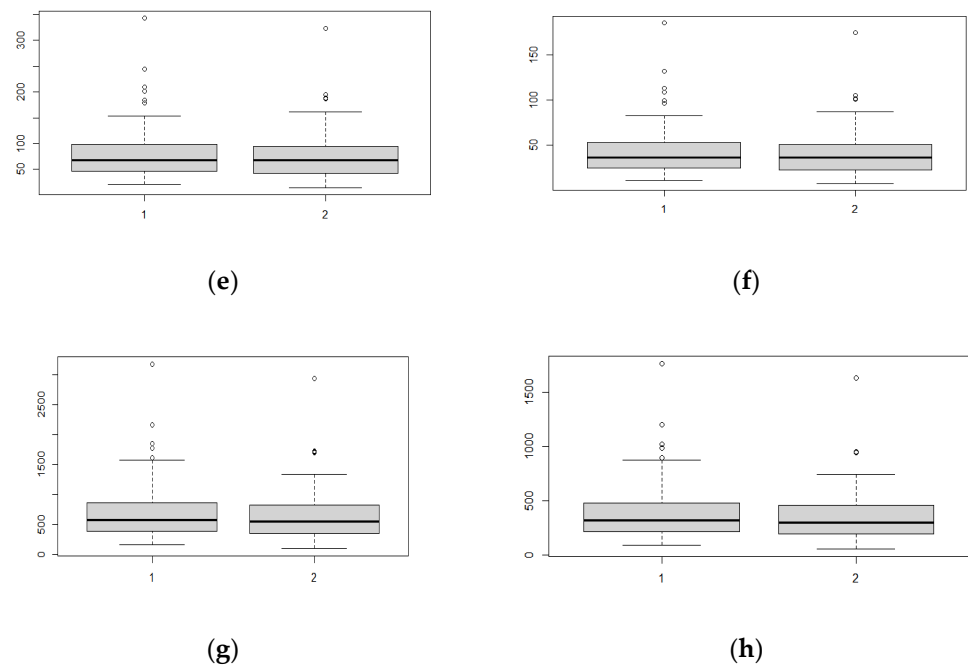


**Figure 7.** (a) Boxplot of circumference at 1.30 m (cm) measured and estimated with field data collection (1) and from UAV-ALS-TLS data (2), (b) boxplot of tree height (m) measured and estimated with field data collection (1) and from UAV-ALS-TLS data (2), (c) boxplot of aboveground biomass (kg) measured and estimated with field data collection (1) and from UAV-ALS-TLS data (2), (d) boxplot of aboveground carbon stock (kg) measured and estimated with field data collection (1) and from UAV-ALS-TLS data (2), (e) boxplot of belowground biomass (kg) measured and estimated with field data collection (1) and from UAV-ALS-TLS data (2), (f) boxplot of belowground carbon stock (kg) measured and estimated with field data collection (1) and from UAV-ALS-TLS data (2), (g) boxplot of Total biomass (kg) measured and estimated with field data collection (1) and from UAV-ALS-TLS data (2), and (h) boxplot of Total carbon stock (kg) measured and estimated with field data collection (1) and from UAV-ALS-TLS data (2).

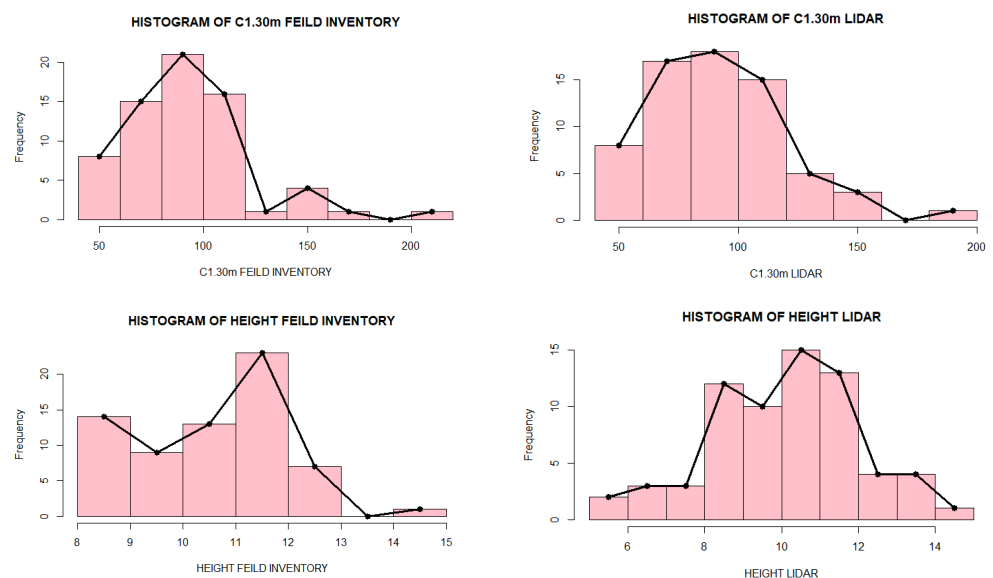


**Figure 8.** Histograms distribution of tree height (m) and circumference at 1.30 m (cm) measured by field data collection and those extracted from UAV-ALS and TLS data (Lidar).

The  $p$ -values from the Shapiro–Wilk test (Table 4) confirm that the circumference at 1.30 m, the tree height measured by the field data collection, and the circumference at 1.30 m extracted by ALS-UAV-TLS data do not follow a normal distribution, except for the tree height extracted from ALS-UAV-TLS data. To compare the means of the two methods, a non-parametric test was used (Wilcoxon-test). The  $p$ -values of this test (Table 4) showed that the means of the circumference at 1.30 m and tree height derived from the two methods are not significantly different (since we rejected the null hypothesis of normality for both distributions at the 5% significance level).

**Table 4.** Shapiro–Wilk test of dendrometric parameters (H, C1.30m), biomass, and carbon stock (aboveground, belowground, and total) measured and estimated with field data collection and from UAV-ALS-TLS data. Wilcoxon test between dendrometric parameters (H, C1.30m), biomass, and carbon stock (aboveground, belowground, and total) measured and estimated with field data collection and from UAV-ALS-TLS data.

Shapiro-Test			
		W	$p$ -Value
C1.30m (cm)	Field measurements	0.9181	0.0002995
	ALS-UAV-TLS	0.95394	0.0145
Height field (m)	Field measurements	0.94178	0.003553
	ALS-UAV-TLS	0.98596	0.6532
$B_{\text{tree-AGB}}$ field (kg)	Field measurements	0.7748	$9.217 \times 10^{-9}$
	ALS-UAV-TLS	0.81877	$1.269 \times 10^{-7}$
$B_{\text{tree-BLG}}$ field (kg)	Field measurements	0.78662	$1.804 \times 10^{-8}$
	ALS-UAV-TLS	0.83436	$3.529 \times 10^{-7}$
$B_{\text{tree-total}}$ field (kg)	Field measurements	0.77616	$9.944 \times 10^{-9}$
	ALS-UAV-TLS	0.82049	$1.417 \times 10^{-7}$
$C_{\text{st-AGB}}$ field (kg)	Field measurements	0.77443	$9.03 \times 10^{-9}$
	ALS-UAV-TLS	0.81842	$1.241 \times 10^{-7}$
$C_{\text{st-BLG}}$ field (kg)	Field measurements	0.78662	$1.804 \times 10^{-8}$
	ALS-UAV-TLS	0.83436	$3.529 \times 10^{-7}$
$C_{\text{tree-total}}$ field (kg)	Field measurements	0.77579	$9.741 \times 10^{-9}$
	ALS-UAV-TLS	0.82013	$1.384 \times 10^{-7}$
Wilcoxon-test			
Field C1.30m (cm)/ C1.30m ALS-UAV-TLS (cm)		2308	0.7792
Field height (m)/Height ALS-UAV-TLS (m)		2605	0.1091
$B_{\text{tree-AGB}}$ field (kg)/ $B_{\text{tree-AGB}}$ ALS-UAV-TLS (kg)		2335	0.6888
$B_{\text{tree-BLG}}$ field (kg)/ $B_{\text{tree-BLG}}$ ALS-UAV-TLS (kg)		2308	0.7792
$B_{\text{st-total}}$ field (kg)/ $B_{\text{st-total}}$ ALS-UAV-TLS (kg)		2328	0.7119
$C_{\text{tree-AGB}}$ field (kg)/ $C_{\text{tree-AGB}}$ ALS-UAV-TLS (kg)		2335	0.6888
$C_{\text{tree-BLG}}$ field (kg)/ $C_{\text{tree-BLG}}$ ALS-UAV-TLS (kg)		2308	0.7792
$C_{\text{st-total}}$ field (kg)/ $C_{\text{st-total}}$ ALS-UAV-TLS (kg)		2329	0.7085

- Aboveground, belowground, and total biomass

The statistical analysis of the aboveground, belowground, and total biomass of each tree showed that the two methods (field data collection and data acquisition by ALS-UAV-TLS) provided close averages with respective values of 619.9 kg and 586.80 kg for the



aboveground biomass, 81.75 kg and 78.46 kg for the belowground biomass, and 701.7 kg and 665.3 kg for the total biomass. Other descriptive statistics of the tree biomasses, obtained by the two methods, are shown in Table 3.

The representation via histogram used to study the data distribution of the aboveground, belowground, and total biomass, calculated with inputs derived from the field measurements and those extracted from the UAV-ALS-TLS data, shows that the data do not seem to follow a normal distribution (Figure 9). The  $p$ -values of the Shapiro–Wilk tests (Table 4), confirm this result (since we rejected the null hypothesis of normality for both distributions at the 5% significance level).

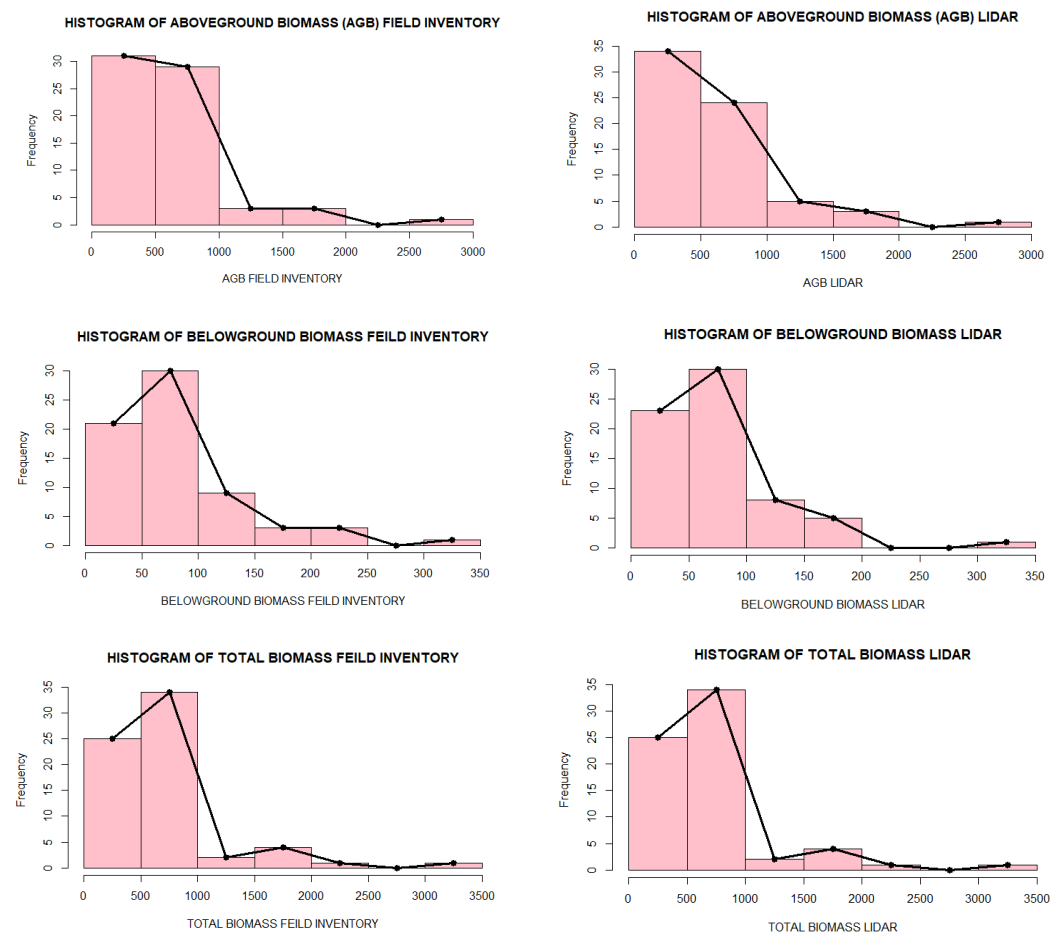


**Figure 9.** Histograms distribution of aboveground, belowground, and total biomass (kg) calculated with two types of inputs (forest parameters from field data collection and those extracted from UAV-ALS and TLS data (Lidar)).

To compare the means of the two methods, a non-parametric test was used (Wilcoxon-test). The  $p$ -values of this test (Table 4) showed that the means of the aboveground, belowground, and total biomass derived from the two methods are not significantly different (since we rejected the null hypothesis of normality for both distributions at the 5% significance level).

- Aboveground, belowground, and total carbon stock

The quantification of the aboveground, belowground, and total carbon stock of each tree showed that the two methods (field data collection and data acquisition by ALS-UAV-TLS) yielded close averages with values of 345.86 kg and 327.39 for the aboveground carbon stock, 44.14 kg and 42.36 kg for the belowground carbon stock, and 390.00 kg and 369.75 kg for the total carbon stock. Other descriptive statistics of the trees' carbon stock, obtained by the two methods, are shown in Table 3.

The representation via histograms (used to study the data distribution of the aboveground, belowground, and total carbon stock, calculated from equations detailed in the Materials and Methods section) show that distributions of the data do not seem to follow a normal distribution (Figure 10). The  $p$ -values of the Shapiro–Wilk tests (Table 4) confirm this result (since we rejected the null hypothesis of normality for both distributions at the 5% significance level).

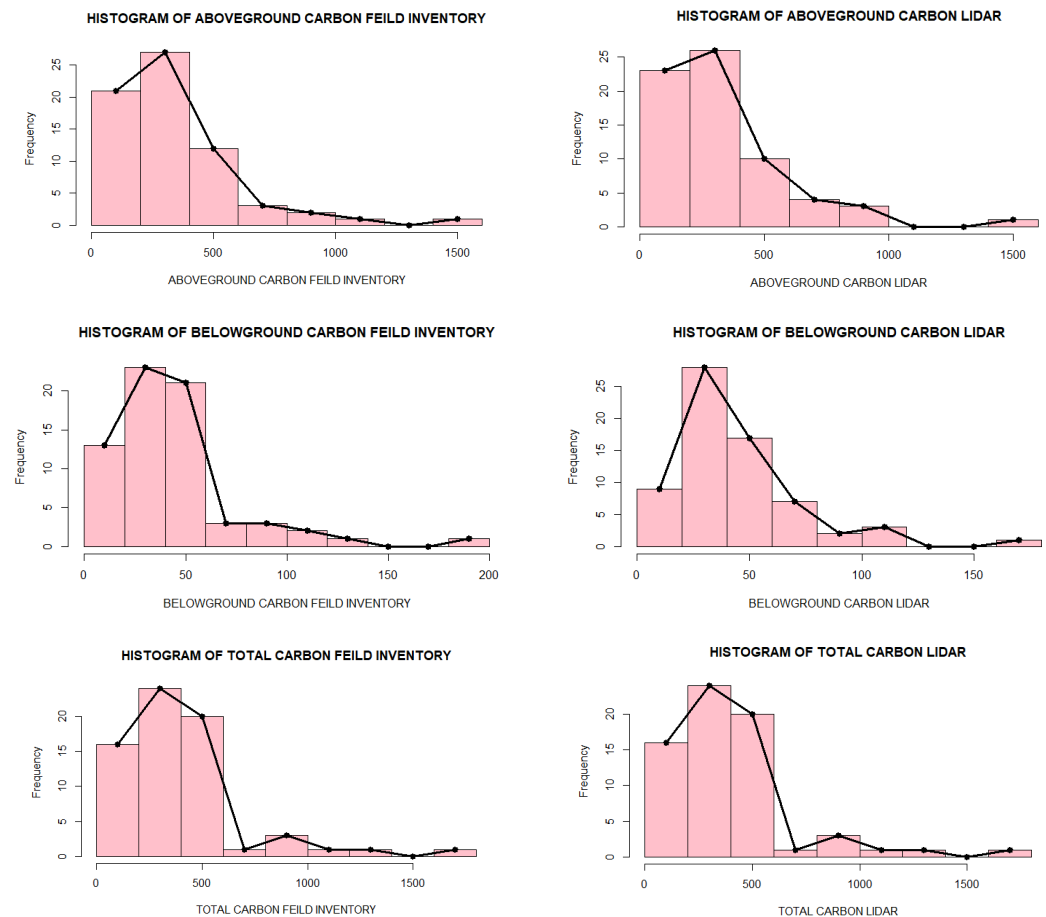


**Figure 10.** Histogram distributions of aboveground, belowground, and total carbon stock (kg) calculated with two types of inputs (forest parameters from field measurements and those extracted from UAV-ALS and TLS data (Lidar)).

To compare the means of the two methods, a non-parametric test was used (Wilcoxon-test). The  $p$ -values of this test (Table 4) showed that the means of the aboveground, belowground, and total carbon stock derived from the two methods are not significantly different (since we rejected the null hypothesis of normality for both distributions at the 5% significance level).

### 3.2.2. Relationship between Dendrometric Parameters, Biomass, and Carbon Stock of the Two Methods (Pearson Correlation, RMSE and Regression Analysis)

A total of 67 trees were used to assess the relationship between the parameters (C1.30m and tree height), biomass, and carbon stock measured in the field measurements and those extracted from the ALS-UAV-TLS data. Therefore, we have used a linear regression with a logarithmic transformation to remedy the abnormal distribution of data.

- C1.30m and tree height

The results show a strong relationship between tree height and circumference at 1.30 m calculated with the two methods (field data collection and ALS-UAV-TLS data), with a

coefficient of Pearson correlation equal to 0.86 and 0.83, respectively. Thus, the root mean square error (RMSE) is equal to 1.84 cm for the circumference at 1.30 m and 0.47 m for the tree height (Table 5).

**Table 5.** Relationship between dendrometric parameters (H, C1.30m), biomass, and carbon stock (aboveground, belowground, and total) measured and estimated with field measurements and from UAV-ALS-TLS data (Pearson Coefficient and RMSE).

	Pearson Coef	RMSE
C1.30m (cm) field/C1.30m ALS-UAV-TLS (cm)	0.86	1.84
Height (m) field/Height ALS-UAV-TLS (m)	0.83	0.47
B <sub>tree-AGB</sub> field (kg)/B <sub>tree-AGB</sub> ALS-UAV-TLS (kg)	0.77	33.11
B <sub>tree-BLG</sub> field (kg)/B <sub>tree-BLG</sub> ALS-UAV-TLS (kg)	0.78	3.29
B <sub>tree-total</sub> field (kg)/B <sub>tree-total</sub> ALS-UAV-TLS (kg)	0.77	36.40
C <sub>tree-AGB</sub> field (kg)/C <sub>tree-AGB</sub> ALS-UAV-TLS (kg)	0.77	18.47
C <sub>tree-BLG</sub> field (kg)/C <sub>tree-BLG</sub> ALS-UAV-TLS (kg)	0.78	1.77
C <sub>st-total</sub> field (kg)/C <sub>st-total</sub> ALS-UAV-TLS (kg)	0.77	20.24

The scatter plots (Figure 11) and Table 6 show a strong relationship with a coefficient of determination ( $R^2$ ) equal to 0.81 and 0.71 for the circumference at 1.30 m and tree height calculated with the two methods (field data collection and ALS-UAV-TLS data), respectively.

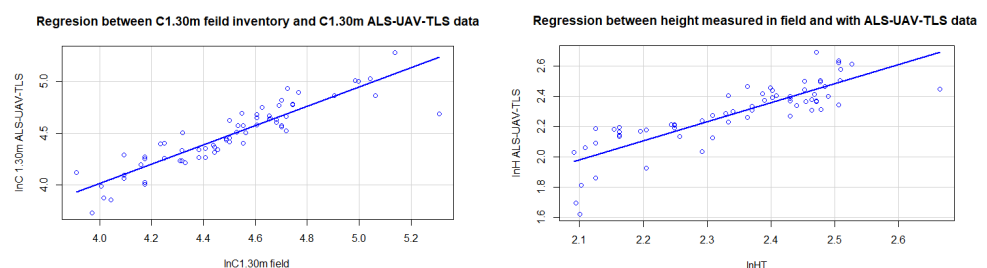


**Figure 11.** Relationship between C1.30m and tree heights measured in the field and those extracted from ALS-UAV-TLS data, represented using linear regression with logarithmic transformation.

**Table 6.** Relationship between dendrometric parameters (H, C1.30m), biomass, and carbon stock (aboveground, belowground, and total) measured and estimated with field measurements and from UAV-ALS-TLS data using linear regression with a logarithmic transformation.

Dendrometric Parameters				
	Multiple $R^2$			Adjusted $R^2$
lnC1.30m field/lnC1.30m ALS-UAV-TLS	0.818			0.815
lnHeight field/lnHeight ALS-UAV-TLS	0.712			0.708
	Estimate	Std. Error	t Value	Pr(> t )
Intercept1	0.28266	0.24605	1.149	0.255
lnC1.30m field	0.93247	0.05455	17.093	$<2 \times 10^{-16}$ ***
Intercept2	−0.65355	0.23238	−2.812	0.0065 **
lnHeight field	1.25423	0.09885	12.689	$<2 \times 10^{-16}$ ***

Table 6. Cont.

Aboveground, belowground, and total Biomass				
	Multiple R <sup>2</sup>		Adjusted R <sup>2</sup>	
lnB <sub>tree-AGB field</sub> /lnB <sub>tree-AGB ALS-UAV-TLS</sub>	0.833		0.831	
lnB <sub>tree-BLG field</sub> /lnB <sub>tree-BLG ALS-UAV-TLS</sub>	0.818		0.8152	
lnB <sub>tree-total field</sub> /lnB <sub>tree-total ALS-UAV-TLS</sub>	0.832		0.829	
	Estimate	Std. Error	t value	Pr(> t )
Intercept1	0.18394	0.33292	0.553	0.583
lnB <sub>tree-AGB field</sub>	0.96027	0.05322	18.044	<2 × 10 <sup>−16</sup> ***
Intercept2	0.24263	0.23259	1.043	0.301
lnB <sub>tree-BLG field</sub>	0.93247	0.05455	17.093	<2 × 10 <sup>−16</sup> ***
Intercept3	30.21400	0.34009	0.629	0.531
lnB <sub>tree-total field</sub>	0.95675	0.05329	17.953	<2 × 10 <sup>−16</sup> ***
Aboveground, belowground, and total carbon stock				
	Multiple R <sup>2</sup>		Adjusted R <sup>2</sup>	
lnC <sub>tree-AGB field</sub> /lnC <sub>tree-AGB ALS-UAV-TLS</sub>	0.8335		0.831	
lnC <sub>tree-BLG field</sub> /lnC <sub>tree-BLG ALS-UAV-TLS</sub>	0.712		0.708	
lnC <sub>st-total field</sub> /lnC <sub>st-total ALS-UAV-TLS</sub>	0.8321		0.8296	
	Estimate	Std. Error	t value	Pr(> t )
Intercept1	0.16194	0.30202	0.536	0.594
lnC <sub>tree-AGB field</sub>	0.96006	0.05322	18.040	<2 × 10 <sup>−16</sup> ***
Intercept2	0.20102	0.19935	1.008	0.317
lnC <sub>tree-BLG field</sub>	0.93247	0.05455	17.093	<2 × 10 <sup>−16</sup> ***
Intercept3	0.18904	0.30893	0.612	0.543
lnC <sub>st-total field</sub>	0.95667	0.05329	17.951	<2 × 10 <sup>−16</sup> ***

The symbols \*\* and \*\*\* represent the significance code. In the summary of a regression model the significance code is a measure of its *p*-value variation. The range of *p*-value for \*\* is (0.001, 0.01]. The range of *p*-value for \*\*\* is [0, 0.001].

- Aboveground, belowground, and total biomass

The results reveal important relationships, with a Pearson coefficient equal to 0.77, 0.78, and 0.77 and a root mean square error (RMSE) equal to 33.11 kg, 3.29 kg, and 36.4 kg, for the aboveground, belowground, and total biomass, respectively (Table 5).

The scatter plots (Figure 12) and Table 6 shows a strong relationship with a coefficient of determination (R<sup>2</sup>) equal to 0.83, 0.81, and 0.83 for the aboveground, belowground, and total biomass, respectively.

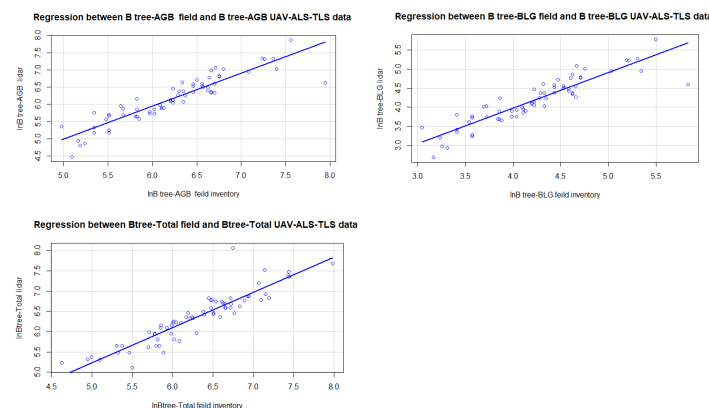


**Figure 12.** Relationship Representation between aboveground, belowground, and total biomass calculated with two types of inputs (forest parameters from field measurements and those extracted from UAV-ALS and TLS data), using linear regression with logarithmic transformation.

- Aboveground, belowground, and total carbon stock

The results deduced important relationships, with a Pearson coefficient equal to 0.77, 0.78, and 0.77 and a root mean square error (RMSE) equal to 18.47 kg, 1.77 kg, and 20.24 kg for the aboveground, belowground, and total carbon stock, respectively (Table 5).

The scatter plots (Figure 13) and Table 6 show a strong relationship with a coefficient of determination ( $R^2$ ) equal to 0.83, 0.81, and 0.83 for the aboveground, belowground, and total carbon stock, respectively.

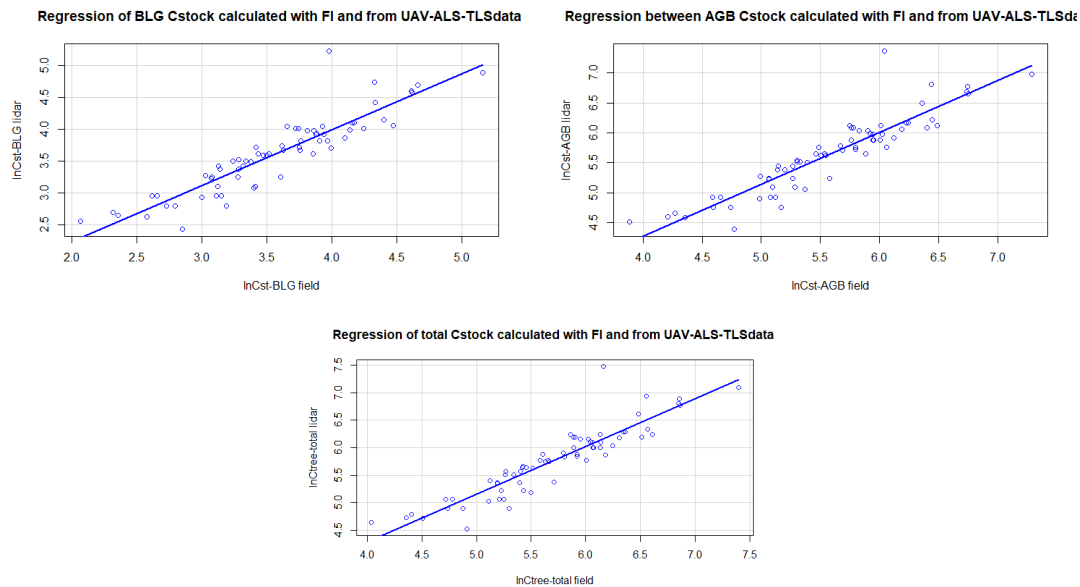


**Figure 13.** Relationship between aboveground, belowground, and total carbon stock calculated with two types of inputs (forest parameters from field measurements and those extracted from UAV-ALS and TLS data), represented using linear regression with logarithmic transformation.

### 3.3. Analysis at Plot Level of Aboveground, Belowground and Total Biomass and Carbon Stock

After having analyzed the biomass and the carbon stock (aboveground, belowground, and total) per tree, we studied the estimation of these parameters at the plot scale (Figure 14) to obtain an idea of the biomass and carbon stock of the cork oak stand. The table below (Table 7) presents the biomass and the carbon stock (aboveground, belowground, and total) of each plot and their mean, minimum, and maximum in the studied plots (six plots), calculated with the two methods (field measurements and ALS-UAV-TLS data).

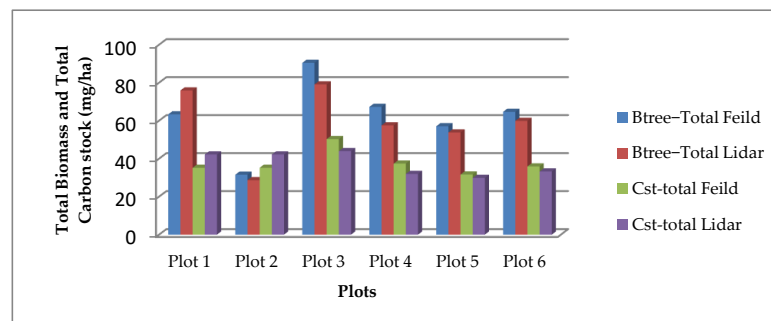


**Figure 14.** Total Biomass and carbon stock (Mg/ha) for the six plots. Where  $B_{tree-Total} \text{ Field}$  is the total plot biomass, estimated in the basis of data field, in Mg/ha,  $B_{tree-Total} \text{ Lidar}$  is the total plot biomass, estimated in the basis of ALS-UAV-TLS data,  $C_{st-total} \text{ Field}$  is the total plot carbon stock, estimated in the basis of data field in Mg/ha and  $C_{st-total} \text{ Lidar}$  is the total plot carbon stock, estimated in the basis of ALS-UAV-TLS data in Mg/ha.



**Table 7.** Aboveground, belowground, and total biomass and carbon stock (Mg/ha) by plot and their mean, minimum, and maximum in the six plots. Where  $B_{\text{tree-AGB}}$  is the plot Aboveground biomass in Mg/ha,  $B_{\text{tree-BLG}}$  is the plot belowground biomass in Mg/ha,  $B_{\text{tree-Total}}$  is the total plot biomass in Mg/ha,  $C_{\text{st-AGB}}$  is the plot Aboveground carbon stock in Mg/ha,  $C_{\text{st-BLG}}$  is the plot carbon stock in the belowground tissues and  $C_{\text{st-total}}$  is the total plot carbon stock in Mg/ha.

	$B_{\text{tree-AGB}}$ Feild	$B_{\text{tree-BLG}}$ Feild	$B_{\text{tree-Total}}$ Feild	$C_{\text{st-AGB}}$ Feild	$C_{\text{st-BLG}}$ Feild	$C_{\text{st-total}}$ Feild	$B_{\text{tree-AGB}}$ Lidar	$B_{\text{tree-BLG}}$ Lidar	$B_{\text{tree-Total}}$ Lidar	$C_{\text{st-AGB}}$ Lidar	$C_{\text{st-BLG}}$ Lidar	$C_{\text{st-total}}$ Lidar
Plot 1	56.02	7.31	63.33	31.26	3.94	35.21	67.16	8.73	75.89	37.49	4.71	42.20
Plot 2	27.86	3.69	31.55	15.54	3.94	35.21	25.26	3.44	28.70	37.49	4.71	42.20
Plot 3	80.19	10.26	90.45	44.76	5.54	50.30	69.95	9.16	79.10	39.04	4.94	43.98
Plot 4	59.45	7.81	67.26	33.18	4.22	37.40	50.71	6.79	57.51	28.30	3.67	31.97
Plot 5	50.19	6.86	57.05	27.98	3.71	31.68	47.19	6.60	53.79	26.31	3.56	29.87
Plot 6	56.98	7.68	64.66	31.77	4.15	35.92	52.75	7.14	59.89	29.41	3.85	33.27
Mean	55.11	7.27	62.38	30.74	4.25	37.62	52.17	6.98	59.15	33.01	4.24	37.25
Min	27.86	3.69	31.55	15.54	3.71	31.68	25.26	3.44	28.70	26.31	3.56	29.87
Max	80.19	10.26	90.45	44.76	5.54	50.30	69.95	9.16	79.10	39.04	4.94	43.98

Based on the values of Table 7 and Figure 14, we conclude that the means of the aboveground, belowground, and total biomass calculated with the two types of input (forest parameters from the field data collection and those extracted from UAV-ALS-TLS data) are very close, yielding (55.11; 52.17 Mg/ha), (7.27; 6.98 Mg/ha), and (62.38; 59.15 Mg/ha). In addition, the means of the aboveground, belowground, and total carbon stock calculated with the two methods are also very close, yielding (30.74; 33.01 Mg/ha), (4.25; 4.24 Mg/ha), and (37.62; 37.25 Mg/ha).

#### 4. Discussion

Biomass and carbon stock estimations using new technologies (ALS, UAV, and TLS) have been performed using different methodologies in previous research. The new approach that we have proposed in this study, consisting of a combination of 3D clouds of ALS and TLS at the plot level, has rarely been applied in other studies. So, the comparison of our results is made, on the one hand, with results from research using conventional methods, and on the other hand, with research using Lidar (Aerial or Terrestrial), alone or combined with other remote sensing tools.

##### 4.1. Dendrometric Parameters (Tree Height and Circumference at 1.30 m)

The estimation of tree heights and circumference at 1.30 m are very important because they constitute the inputs of allometric equations used for the estimation of biomass and carbon stock. The determination of these dendrometric parameters depends among other things on the tree segmentation method (algorithm segmentation), which must be adapted to the nature of the study stand [43].

The statistical analysis results of the circumference at 1.30 m with the two methods (field data and ALS-UAV-TLS data) show a very strong relationship, with an  $R^2$  equal to 0.81, a Pearson coefficient equal to 0.86, and RMSE equal to 1.84 cm. This corresponds to the results of [32], where the researchers found that the DBH measured in the field is highly related to that extracted from the TLS with an  $R^2$  equal to 0.98 and an RMSE equal to 1.48 cm, and those of [44], with an  $R^2$  equal to 0.96.

In addition, the results deduced for the tree height, when comparing the two methods (field data and ALS-UAV-TLS data), present an  $R^2$  equal to 0.71, a Pearson coefficient equal to 0.83, and an RMSE equal to 0.47 m, which is very close to the results concluded in the Ayer Hitam Forest Reserve Malaysia, where an  $R^2$  equal to 0.98 was obtained and with no significance difference between the height measured from the field data collection and the one estimated from Lidar data [45]. Others results deduced that there is an important

relationship between manually obtained and ground-based Lidar (TLS) tree heights, with an  $R^2$  equal to 0.79 for [44] and to 0.69 for [32].

#### 4.2. Estimation of Aboveground, Belowground, and Total Biomass

The application of allometric equations to estimating biomass (aboveground and belowground) is the best method since it enables an estimation of the biomass without destructing forests. Nevertheless, data acquisition by conventional field data collection in a large area is painful and time consuming, hence the interest of using the new technologies (ALS-UAV and TLS). The choice of the appropriate allometric equation is not evident and largely influences the results. In our study area, unfortunately, little research has concerned this aspect and there is no direct allometric equation for estimating biomass. So, to estimate biomass on the basis of the two types of inputs, we first calculated the volume and then the biomass of cork and stems with coarse branches, and we used direct equations for the other parts of the tree (medium and small branches, foliage, and roots) established for cork oak trees in Spain.

The proposed method (ALS-UAV-TLS data acquisition) provides more accurate results for biomass estimation compared to field data, with an  $R^2$  equal to 0.82, a Pearson coefficient equal to 0.77, and an RMSE equal to 36.4 kg. This result has been confirmed by many researchers, with an  $R^2$  equal to 0.93 in [46], and an  $R^2$  ranging from 0.68 to 0.85 depending on the species [47].

The values of the aboveground biomass per tree ranged from 145.47 to 2826.86 kg (mean value of 619.9 kg) for the field data and from 87.8 to 2609.16 kg (mean value of 586.79 kg) for the ALS-UAV-TLS data. These values are close to those concluded by [40] for the Maamora forest (26 to 2177 kg with a mean value of 379 kg), by [41] for another cork oak Moroccan forest (11 to 1255 kg), and by [42] for a Spanish cork oak forest (11 to 2412 kg with mean value of 512 kg).

The aboveground biomass of cork oak stand varies from 27.86 to 80.18 Mg/ha (mean of 55.11 Mg/ha) for the field data and from 25.26 to 69.94 Mg/ha (mean value of 52.17) for ALS-UAV-TLS data, which is very close to the 64.27 Mg/ha concluded in the same forest [40], where the stand has a density of less than 100 stem/ha, and is fairly comparable to the 34 and 183 Mg/ha for *Quercus ilex* stands in the high and middle Atlas mountains in Morocco, respectively [48].

The results concerning the belowground biomass per tree range between 21.2 and 343.08 kg (mean value of 81.74 kg) for the field data and between 14.66 and 322.79 kg (mean value of 78.45 kg) for the ALS-UAV-TLS data.

The belowground biomass of the cork oak stand varies from 3.69 to 10.26 Mg/ha (mean value of 7.2 Mg/ha), equivalent to 11.65% of the total tree biomass, for the field data and from 3.43 to 9.15 Mg/ha (mean value of 6.97 Mg/ha), which is equivalent to 11.73%, for the ALS-UAV-TLS data. These results fairly overlap with those obtained in [40], representing 10 Mg/ha, the equivalent to 14% of the total tree biomass, and are thus close to the lower values reported for deciduous species (10–49%) [42,49].

The values of tree total biomass of the cork oak stand are equal to 62.38 Mg/ha for the field data and 59.14 Mg/ha for the ALS-UAV-TLS data, which are very close to the 74.27 Mg/ha concluded in the same forest [40], where the stand has a density less than 100 stem/ha.

#### 4.3. Estimation of Aboveground, belowground, and total Carbon Stock

The results show that the method proposed in this study, consisting in the collection of data with ALS-UAV at the top of the stand and multiscan TLS within the cork oak stand, provides accurate forest parameters that are very close to those measured in the field; in fact, the Wilcoxon-test demonstrated that the means of the circumference at 1.30 m and tree height derived from the two methods are not significantly different ( $p = 5\%$ ).

This accuracy in the determination of the dendrometric parameters is reflected in the results obtained for the estimation of the biomass and carbon stock. The ALS-UAV-TLS data

could accurately estimate carbon stock compared to the traditional forest data collection method, with a Pearson coefficient of 0.77, an  $R^2$  of 0.83, and an RMSE of 20.24 kg.

In this study, the aboveground carbon stock per tree varied from 80.96 to 1579.41 kg (mean value of 345.86 kg) for the field data and from 48.89 to 1457.79 kg (mean value of 327.39 kg) for the ALS-UAV-TLS data.

The values of aboveground carbon stock of Cork oak stand ranged between 27.97 and 44.76 Mg/ha (mean value of 33.36 Mg/ha) for the field data and between 26.3 and 39.04 Mg/ha (mean value of 33 Mg/ha) for the ALS-UAV-TLS data. These results are very close to those resulting in the same forest [40]; in fact, for the stand with a density less than 100 stem/ha, the values of the aboveground carbon stock are ranged between 21.3 and 58 Mg/ha (mean value of 35.8 Mg/ha). In addition, the observed range compares well with species of the same genus, such as *Quercus ilex* (17–91 Mg/ha) [48].

#### 4.4. Biomass and Carbon Stock in the Cork Oak Stand

The use of data from an ALS onboard a UAV and the TLS provide interesting results with respect to the quantification of biomass and carbon stock with more precision and a greater economy of time and effort. In fact, the quantification of the biomass and carbon stock in the Maamora Cork Oak stand using these two methods yields very close values ranging between 27.86 to 80.18 Mg/ha (mean of 55.11 Mg/ha) for the field data and from 25.26 to 69.94 Mg/ha (mean value of 52.17) for the ALS-UAV-TLS data, respectively, and between 27.97 and 44.76 Mg/ha (mean value of 33.36 Mg/ha) for the field data and between 26.3 and 39.04 Mg/ha (mean value of 33 Mg/ha) for the ALS-UAV and TLS data, respectively. These low values of biomass and carbon stock are explained by the state of the degradation of this forest, which is the result of the combined effect of several factors (natural and anthropogenic) and by the low density of the population in the study area.

In effect, the biomass and carbon stock per cork oak tree in the study area are relatively high but given that the number of stems per hectare is low this results in a low biomass and carbon stock per hectare. So, in order to increase the contribution of this forest towards carbon sequestration and the fight against climate change, it is significantly important and stimulating to program the artificial regeneration of cork oak, to reforest sylvopastoral species, and to create other sources of income, all in an effort to reduce anthropogenic pressure.

The results show that the biomass and carbon stock (aboveground, belowground, and total) extracted from ALS-UAV-TLS data are more consistent with the reference values based on the field survey data. This confirms the conclusions of numerous studies that had experimented with the use of airborne or terrestrial Lidar, alone or combined with other remote sensing tools, towards the estimation of the biomass and the carbon stock either at the tree level or at the forest stand level.

The objective of our work was to estimate the biomass and the carbon stock at the tree and plot scales. Furthermore, it would be very interesting to quantify and map biomass and carbon stock over large areas. This is in line with the prospects of our future work. Indeed, to map the biomass and carbon stock over a large area, we will perform another methodology, using regression analysis between the plots' values of biomass and carbon stock calculated by forest inventory and metrics extracted from UAV-ALS-TLS data on the one hand and with metrics extracted from satellite images on the other.

## 5. Conclusions

In this study, our main goal was to estimate the biomass and carbon stock in a cork oak forest using a new approach based on the combination of Aerial laser scanning carried by Unmanned Aerial Vehicle (ALS-UAV) and Terrestrial laser scanning (TLS) data and to compare their results with those of field measurements. To achieve this goal, we collected data via an ALS scan of the entire area, a multiscan TLS, and field data collection at the plot level. Then, we proceeded to the automatic extraction of the dendrometric parameters of all the existing trees in the study area. These dendrometric parameters (tree height

and circumference at 1.30 m) served as inputs for the allometric equations used in the biomass and carbon stock (aboveground, belowground, and total) estimation. The results of the statistical analysis show that the proposed approach provides very interesting results compared to the field data, with a considerable reduction in time and effort. The results show that the ALS-UAV-TLS data could accurately estimate biomass and carbon stock compared to the field data, with a Pearson coefficient of 0.77, an  $R^2$  of 0.83, and an RMSE of 36.40 kg for the biomass and 20.24 kg for the carbon stock. The low values of biomass and carbon stock in the cork oak stand of the Maamora forest reflect this forest's state of degradation. Thus, this study can provoke interest in future studies of the degradational aspects and the carbon stock changes over time with respect to this forest and its contribution in the fight against climate change, using satellite images and new technologies such as UAVs, ALS, and TLS.

**Author Contributions:** Conceptualization, F.S., S.I. and B.M.; Formal analysis, F.S., S.I. and M.K.; Methodology, F.S., S.I., B.M. and A.E.k.K.; Project administration, S.I.; Software, S.I., A.E.k.K., K.S., H.L. and M.K.; Validation, S.I., B.M. and A.E.k.K.; Visualization, F.S., S.I., B.M., A.E.k.K. and H.L.; Writing—original draft, F.S.; Writing—review & editing, F.S., S.I. and M.K. All authors have read and agreed to the published version of the manuscript.

**Funding:** This research received no external funding.

**Acknowledgments:** The authors express their gratitude to the company AXIGEO for their provision of UAV-LiDAR equipment, and to the company Prime Zeone Systemes for providing the TLS equipment. We also acknowledge El Ghoudani Driss, El Mderssa Mohamed and Mohamed El Hanafi for their valuable contribution in the field data acquisition.

**Conflicts of Interest:** The authors declare that they have no known competing financial interests or personal relationships that could have appeared to influence the work reported in this paper.

## Appendix A

$$V_{\text{tree}} = 0.6 (C1.30m)^{2.18} \quad (A1)$$

where  $V_{\text{tree}}$  is the tree volume of wood, thick branches, and cork (in  $m^3$ ), and C1.30m the circumference at 1.30 m (in m).

$$V_{\text{cork}} = 0.0151 (C1.30m)^{1.9827} \quad (A2)$$

$$V_{\text{stem-bigB}} = V_{\text{tree}} - V_{\text{cork}} \quad (A3)$$

where  $V_{\text{stem-bigB}}$  is the volume of the stem with coarse branches (in  $m^3$ ),  $V_{\text{cork}}$  is the volume of the cork (in  $dm^3$ ), C1.30m the circumference at 1.30 m (in cm), and  $V_{\text{tree}}$  is the tree volume of wood, thick branches, and cork (in  $m^3$  from Equation (A1)).

$$B_{\text{cork}} = V_{\text{cork}} \times D \quad (A4)$$

$$B_{\text{stem-bigB}} = V_{\text{stem-bigB}} \times D \quad (A5)$$

where  $B_{\text{cork}}$  is the biomass of cork (kg),  $V_{\text{cork}}$  is the volume of cork ( $m^3$ ),  $B_{\text{stem-bigB}}$  is the biomass of the stem and coarse branches without bark (kg),  $V_{\text{stem-bigB}}$  is the volume of the stem with coarse branches ( $m^3$ ), and D is the specific tissue density (Table A1).

**Table A1.** Specific tissue density and mean carbon concentration of the tissues adapted from [40].

	Specific Tissue Density (kg m <sup>−3</sup> )	Mean Carbon Concentration (g/kg)
Stem and Coarse branches (Ø > 10 cm)	830	560
Cork	540	560
Medium branches (2 ≤ Ø ≤ 10 cm)	-	540
Small branches (Ø < 2 cm)	-	530
Foliage	-	520
Roots	-	

$$B_{\text{tree-BLG}} = 0.0829 \cdot D_{1.30\text{m}}^2 \quad (\text{A6})$$

where  $B_{\text{tree-BLG}}$  is the belowground biomass of an individual tree in kg and  $D_{1.30\text{m}}$  is the diameter at breast height (1.30 m) in cm.

## References

- IPCC. Climate Change 2022: Impacts, Adaptation, and Vulnerability. Contribution of Working Group II to the Six Assessment Report of the Intergovernmental Panel on Climate Change. 2022. Available online: <https://www.ipcc.ch/report/ar6/wg2/> (accessed on 4 June 2022).
- Friedlingstein, P.; O’Sullivan, M.; Jones, M.W.; Andrew, R.M.; Hauck, J.; Olsen, A.; Peters, G.P.; Peters, W.; Pongratz, J.; Sitch, S.; et al. Global Carbon Budget 2020. *Earth Syst. Sci. Data* **2020**, *12*, 3269–3340. [CrossRef]
- Harris, N.L.; Gibbs, D.A.; Baccini, A.; Birdsey, R.A.; de Bruin, S.; Farina, M.; Fatoyinbo, L.; Hansen, M.C.; Herold, M.; Houghton, R.A.; et al. Global Maps of Twenty-First Century Forest Carbon Fluxes. *Nat. Clim. Chang.* **2021**, *11*, 234–240. [CrossRef]
- Watson, R.T.; Noble, I.R.; Bolin, B.; Ravindranath, N.H.; Verardo, D.J.; Dokken, D.J. *Land Use, Land-Use Change and Forestry: A Special Report of the Intergovernmental Panel on Climate Change*; Cambridge University Press: Cambridge, UK, 2000.
- Dixon, R.K.; Winjum, J.K.; Andrasko, K.J.; Lee, J.J.; Schroeder, P.E. Integrated Land-Use Systems: Assessment of Promising Agroforest and Alternative Land-Use Practices to Enhance Carbon Conservation and Sequestration. *Clim. Chang.* **1994**, *27*, 71–92. [CrossRef]
- Matyssek, R.; Wieser, G.; Calfapietra, C.; de Vries, W.; Dizengremel, P.; Ernst, D.; Jolivet, Y.; Mikkelsen, T.N.; Mohren, G.M.J.; Le Thiec, D.; et al. Forests under Climate Change and Air Pollution: Gaps in Understanding and Future Directions for Research. *Environ. Pollut.* **2012**, *160*, 57–65. [CrossRef] [PubMed]
- Rappaport, D.I.; Morton, D.C.; Longo, M.; Keller, M.; Dubayah, R.; dos-Santos, M.N. Quantifying Long-Term Changes in Carbon Stocks and Forest Structure from Amazon Forest Degradation. *Environ. Res. Lett.* **2018**, *13*, 065013. [CrossRef]
- Pandey, A.; Arunachalam, K.; Thadani, R.; Singh, V. Forest Degradation Impacts on Carbon Stocks, Tree Density and Regeneration Status in Banj Oak Forests of Central Himalaya. *Ecol. Res.* **2020**, *35*, 208–218. [CrossRef]
- Croitoru, L.; Merlo, M. Mediterranean Forest Values. In *Valuing Mediterranean Forests: Towards Total Economic Value*; CABI Publishing: Wallingford, UK, 2005; pp. 37–68.
- Houghton, J. *Global Warming: The Complete Briefing*; Cambridge University Press: Cambridge, UK, 2009.
- Lu, D. The Potential and Challenge of Remote Sensing-based Biomass Estimation. *Int. J. Remote Sens.* **2006**, *27*, 1297–1328. [CrossRef]
- CDP-Global-Climate-Change-Report-2015. Available online: <https://cdn.cdp.net/cdp-production/cms/reports/documents/000/000/578/original/CDP-global-climate-change-report-2015.pdf> (accessed on 4 June 2022).
- Vashum, K.T. Methods to Estimate Above-Ground Biomass and Carbon Stock in Natural Forests—A Review. *J. Ecosyst. Ecography* **2012**, *2*, 1–7. [CrossRef]
- Liu, C.; Lu, M.; Cui, J.; Li, B.; Fang, C. Effects of Straw Carbon Input on Carbon Dynamics in Agricultural Soils: A Meta-Analysis. *Glob. Change Biol.* **2014**, *20*, 1366–1381. [CrossRef] [PubMed]
- McGovern, M.; Pasher, J. Canadian Urban Tree Canopy Cover and Carbon Sequestration Status and Change 1990–2012. *Urban For. Urban Green.* **2016**, *20*, 227–232. [CrossRef]
- Myeong, S.; Nowak, D.J.; Duggin, M.J. A Temporal Analysis of Urban Forest Carbon Storage Using Remote Sensing. *Remote Sens. Environ.* **2006**, *101*, 277–282. [CrossRef]
- Shen, H.; Huang, L.; Zhang, L.; Wu, P.; Zeng, C. Long-Term and Fine-Scale Satellite Monitoring of the Urban Heat Island Effect by the Fusion of Multi-Temporal and Multi-Sensor Remote Sensed Data: A 26-Year Case Study of the City of Wuhan in China. *Remote Sens. Environ.* **2016**, *172*, 109–125. [CrossRef]
- Jong, S.M.D.; Pebesma, E.J.; Lacaze, B. Above-Ground Biomass Assessment of Mediterranean Forests Using Airborne Imaging Spectrometry: The DAIS Peyne Experiment. *Int. J. Remote Sens.* **2003**, *24*, 1505–1520. [CrossRef]



19. Raciti, S.M.; Huttyra, L.R.; Newell, J.D. Mapping Carbon Storage in Urban Trees with Multi-Source Remote Sensing Data: Relationships between Biomass, Land Use, and Demographics in Boston Neighborhoods. *Sci. Total Environ.* **2014**, *500*–501, 72–83. [CrossRef] [PubMed]
20. Thenkabail, P.S.; Stucky, N.; Griscom, B.W.; Ashton, M.S.; Diels, J.; van der Meer, B.; Enclona, E. Biomass Estimations and Carbon Stock Calculations in the Oil Palm Plantations of African Derived Savannas Using IKONOS Data. *Int. J. Remote Sens.* **2004**, *25*, 5447–5472. [CrossRef]
21. Koch, B. Status and Future of Laser Scanning, Synthetic Aperture Radar and Hyperspectral Remote Sensing Data for Forest Biomass Assessment. *ISPRS J. Photogramm. Remote Sens.* **2010**, *65*, 581–590. [CrossRef]
22. Stephens, P.R.; Kimberley, M.O.; Beets, P.N.; Paul, T.S.H.; Searles, N.; Bell, A.; Brack, C.; Broadley, J. Airborne Scanning LiDAR in a Double Sampling Forest Carbon Inventory. *Remote Sens. Environ.* **2012**, *117*, 348–357. [CrossRef]
23. Fatoyinbo, T.; Feliciano, E.A.; Lagomasino, D.; Lee, S.K.; Trettin, C. Estimating Mangrove Aboveground Biomass from Airborne LiDAR Data: A Case Study from the Zambezi River Delta. *Environ. Res. Lett.* **2018**, *13*, 025012. [CrossRef]
24. Hickey, S.M.; Callow, N.J.; Phinn, S.; Lovelock, C.E.; Duarte, C.M. Spatial Complexities in Aboveground Carbon Stocks of a Semi-Arid Mangrove Community: A Remote Sensing Height-Biomass-Carbon Approach. *Estuar. Coast. Shelf Sci.* **2018**, *200*, 194–201. [CrossRef]
25. Wang, D.; Wan, B.; Liu, J.; Su, Y.; Guo, Q.; Qiu, P.; Wu, X. Estimating aboveground biomass of the mangrove forests on northeast Hainan Island in China using an upscaling method from field plots, UAV-LiDAR data and Sentinel-2 imagery. *Int. J. Appl. Earth Obs. Geoinf.* **2020**, *85*, 101986. [CrossRef]
26. De Almeida, C.T.; Galvao, L.S.; Ometto, J.P.H.B.; Jacon, A.D.; de Souza Pereira, F.R.; Sato, L.Y.; Lopes, A.P.; de Alencastro Graça, P.M.L.; de Jesus Silva, C.V.; Ferreira-Ferreira, J.; et al. Combining LiDAR and Hyperspectral Data for Aboveground Biomass Modeling in the Brazilian Amazon Using Different Regression Algorithms. *Remote Sens. Environ.* **2019**, *232*, 111323. [CrossRef]
27. Longo, M.; Keller, M.; dos-Santos, M.N.; Leitold, V.; Pinagé, E.R.; Baccini, A.; Saatchi, S.; Nogueira, E.M.; Batistella, M.; Morton, D.C. Aboveground Biomass Variability across Intact and Degraded Forests in the Brazilian Amazon. *Glob. Biogeochem. Cycles* **2016**, *30*, 1639–1660. [CrossRef]
28. Tyukavina, A.; Baccini, A.; Hansen, M.C.; Potapov, P.V.; Stehman, S.V.; Houghton, R.A.; Krylov, A.M.; Turubanova, S.; Goetz, S.J. Aboveground Carbon Loss in Natural and Managed Tropical Forests from 2000 to 2012. *Environ. Res. Lett.* **2015**, *10*, 074002. [CrossRef]
29. Wang, V.; Gao, J.; Schwendenmann, L. Assessing Changes of Urban Vegetation Cover and Aboveground Carbon Stocks Using LiDAR and Landsat Imagery Data in Auckland, New Zealand. *Int. J. Remote Sens.* **2020**, *41*, 2140–2158. [CrossRef]
30. Fadil, S.; Sebari, I.; Bouhaloua, M.; Kadi, K.A.E. Opportunités d'utilisation de la technologie drone au niveau des écosystèmes forestiers. *Rev. Maroc. Des Sci. Agron. Vét* **2020**, *8*. Available online: [https://www.agrimaroc.org/index.php/Actes\\_IAPHV2/article/view/888](https://www.agrimaroc.org/index.php/Actes_IAPHV2/article/view/888) (accessed on 4 June 2022).
31. Mtui, Y.P. Tropical Rainforest above Ground Biomass and Carbon Stock Estimation for Upper and Lower Canopies Using Terrestrial Laser Scanner and Canopy Height Model from Unmanned Aerial Vehicle (UAV) Imagery in Ayer-Hitam, Malaysia. Master's Thesis, University of Twente, Enschede, The Netherlands, 2017; p. 73.
32. Fernandes, M.R.; Aguiar, F.C.; Martins, M.J.; Rico, N.; Ferreira, M.T.; Correia, A.C. Carbon Stock Estimations in a Mediterranean Riparian Forest: A Case Study Combining Field Data and UAV Imagery. *Forests* **2020**, *11*, 376. [CrossRef]
33. Wirasatriya, A.; Pribadi, R.; Iryanthony, S.B.; Maslukah, L.; Sugianto, D.N.; Helmi, M.; Ananta, R.R.; Adi, N.S.; Kepel, T.L.; Ati, R.N.A.; et al. Mangrove Above-Ground Biomass and Carbon Stock in the Karimunjawa-Kemujan Islands Estimated from Unmanned Aerial Vehicle-Imagery. *Sustainability* **2022**, *14*, 706. [CrossRef]
34. Belghazi, B.; Ezzahiri, M.; Amhajar, M.; Benzzyane, M. Régénération artificielle du chêne-liège dans la forêt de la Mâamora (Maroc). *For. Méditerran.* **2001**, *22*, 253–261.
35. Aafi, A.; Achhal El Kadmiri, A.; Benabid, A.; Rochdi, M. Richesse et diversité floristique de la subéraie de la Mamora (Maroc). *Acta Bot. Malacit.* **2005**, *30*, 127–138. [CrossRef]
36. Aafi, A. *Etude de la Diversité Floristique de L'écosystème de Chêne-Liège de la Forêt de la Mamora*; Institut Agronomique et Vétérinaire Hassan II: Rabat, Morocco, 2007.
37. Noumonvi, K.D.; Mounir, F.; Belghazi, B. Spatial Multi-Criteria Based Analysis to Assess Dynamics and Vulnerability of Forest Ecosystems to Global Changes: Case of Maamora Forest-Morocco. *OALib* **2017**, *4*, 1–16. [CrossRef]
38. Kankare, V.; Liang, X.; Vastaranta, M.; Yu, X.; Holopainen, M.; Hyypä, J. Diameter Distribution Estimation with Laser Scanning Based Multisource Single Tree Inventory. *ISPRS J. Photogramm. Remote Sens.* **2015**, *108*, 161–171. [CrossRef]
39. Tao, S.; Wu, F.; Guo, Q.; Wang, Y.; Li, W.; Xue, B.; Hu, X.; Li, P.; Tian, D.; Li, C.; et al. Segmenting tree crowns from terrestrial and mobile LiDAR data by 2 exploring ecological theories. *ISPRS J. Photogramm. Remote Sens.* **2015**, *110*, 66–76. [CrossRef]
40. Oubrahim, H.; Boulmane, M.; Bakker, M.; Augusto, L.; Halim, M. Carbon Storage in Degraded Cork Oak (*Quercus Suber*) Forests on Flat Lowlands in Morocco. *IForest—Biogeosci. For.* **2016**, *9*, 125–137. [CrossRef]
41. Makhloufi, M.; Abourouh, M.; El Harchaoui, H. Structure Du Peuplement, Tarifs de Cubage et Essai de Traitements Sylvicoles Dans La Subéraie de Chefchaouen. In *Annales de la Recherche Forestière au Maroc*; National Center of Forestry Research: Rabat, Morocco, 2008; Volume 39, pp. 175–177.
42. Ruiz-Peinado Gertrudix, R.; Montero, G.; Del Rio, M. Biomass Models to Estimate Carbon Stocks for Hardwood Tree Species. *For. Syst.* **2012**, *21*, 42. [CrossRef]

43. Ma, K.; Chen, Z.; Fu, L.; Tian, W.; Jiang, F.; Yi, J.; Du, Z.; Sun, H. Performance and Sensitivity of Individual Tree Segmentation Methods for UAV-LiDAR in Multiple Forest Types. *Remote Sens.* **2022**, *14*, 298. [[CrossRef](#)]
44. Maan, G.S.; Singh, C.K.; Singh, M.K.; Nagarajan, B. Tree Species Biomass and Carbon Stock Measurement Using Ground Based-LiDAR. *Geocarto Int.* **2015**, *30*, 293–310. [[CrossRef](#)]
45. Mohd Zaki, N.A.; Abd Latif, Z.; Zainal, M.Z. Aboveground biomass and carbon stock estimation using double sampling approach and remotely-sensed data. *J. Teknol.* **2016**, *78*. [[CrossRef](#)]
46. Qin, S.; Nie, S.; Guan, Y.; Zhang, D.; Wang, C.; Zhang, X. Forest Emissions Reduction Assessment Using Airborne LiDAR for Biomass Estimation. *Resour. Conserv. Recycl.* **2022**, *181*, 106224. [[CrossRef](#)]
47. Zhao, Y.; Ma, Y.; Quackenbush, L.J.; Zhen, Z. Estimation of Individual Tree Biomass in Natural Secondary Forests Based on ALS Data and WorldView-3 Imagery. *Remote Sens.* **2022**, *14*, 271. [[CrossRef](#)]
48. Boulmane, M.; Makhoulfi, M.; Bouillet, J.-P.; Saint-André, L.; Satrani, B.; Halim, M.; Elantri-Tazi, S. Estimation du stock de carbone organique dans la chênaie verte du Moyen Atlas marocain. *Acta Bot. Gallica* **2010**, *157*, 451–467. [[CrossRef](#)]
49. MacDicken, K.G. A Guide to Monitoring Carbon Storage in Forestry and Agroforestry Projects. 1997, p. 91. Available online: <https://agris.fao.org/agris-search/search.do?recordID=XF2015020398> (accessed on 4 June 2022).